Microchim Acta (2011) 173:85–94
DOI 10.1007/s00604-010-0543-6

ORIGINAL PAPER

Bimetallic nano-structured glucose sensing electrode composed of copper atoms deposited on gold nanoparticles

Hongyan Shi · Zhixin Zhang · Yang Wang · Qingyuan Zhu · Wenbo Song

Received: 28 September 2010 / Accepted: 19 December 2010 / Published online: 6 January 2011

Abstract We describe the preparation and sensing capabilities of a bimetallic electrode consisting of copper atoms deposited on gold nanoparticles (GNPs). The electrode was obtained by first constructing a GNP template on the surface of a glassy carbon electrode by exploiting the hydrogen-bonding interactions between pyridine groups on the surface of the GNPs and the carboxy groups of poly (acrylic acid). GNPs (60 nm in diameter) were homogeneously and densely deposited in the template (as revealed by scanning electron microscopy). The electro-deposition of copper ad-atoms on GNPs occurred at an underpotential and was proven by electrochemical techniques. The presence of GNPs in the template accelerated the deposition at low potential due to its beneficial effect on the rate of electron transfer. The new electrode was studied for its response to glucose. Highly stable and reproducible catalytic activity towards glucose oxidation is observed and attributed to the synergistic catalytic effect of the copper atoms on the surface of the GNPs. The detection limit is as low as 50 nM (at a signal-to-noise ratio of 3), and the response is between 200 nM and 10 mM of glucose.

Keywords GNP template · Hydrogen-bonding · Cu · Electrodeposition · Glucose

Introduction

Currently bimetallic nanostructured materials have fascinated researchers due to their potential applications in various technologically important fields and their unique catalytic, electrocatalytic, electronic, magnetic properties, which differ from their monometallic counterparts. Bimetallic nanostructured systems offer highly dispersed and maximized atomic contacts of their corresponding constituent elements, as well as large catalytic and electrochemical active surface areas that promote both bifunctional and electronic effects. Therefore, bimetallic nanostructured materials often exhibit enhanced electrocatalytic performances in terms of activity, selectivity, and stability compared with their separate components [1]. Fabrication of bimetallic nanostructured materials possessing well-controlled shapes, sizes, chemical composition and structure has recently became a hot topic in areas involving high performance catalysis [2].

Gold nanoparticles (GNPs) have been widely utilized to fabricate different kinds of biosensors by modification of electrode since they have the ability to enhance the electrode conductivity and facilitate the electron transfer, thus, improving the analytical performance [3]. It is well-known that GNPs were often prepared in the presence of suitable stabilizing molecules, with one ends of which either adsorbed or chemically linked to the gold surface. Recent researches demonstrated that the characteristics of

Electronic supplementary material The online version of this article (doi:10.1007/s00604-010-0543-6) contains supplementary material, which is available to authorized users.

H. Shi · Y. Wang · W. Song (✉)
College of Chemistry, Jilin University,
Changchun 130012, China
e-mail: wbsong@jlu.edu.cn

Q. Zhu (✉)
China-Japan Union Hospital of Jilin University,
Changchun 130033, China
e-mail: zhuqy001@163.com

Z. Zhang
The First Hospital of Jilin University,
Changchun 130021, China

GNPs' modified electrode, such as conductivity and electrocatalytic ability, were strongly affected by the chemical reagents surrounding or binding to them [4]. In order to enhance the electrocatalytic activity of the GNPs' modified electrode, efforts were continuously made to modify bimetallic nanostructures on the GNPs' surface based on considerations of the expected synergic effects in electrocatalysis.

Various physical and chemical strategies have been explored to create the GNP-based bimetallic nanostructures films. Among these techniques, electrochemical deposition routes are demonstrated to be superior in many aspects such as low cost, versatility, controllability for almost all metals, and avoidance of complicated separation procedures. Electrodeposition is a low temperature and inexpensive alternative to successive sputtering or annealing-induced segregation for creating another metal skin over a preformed metal core and studying their catalytic properties. The procedures of electrodeposition are simple and controllable with the advantage of avoiding complicated separation procedures in comparison with the wet chemical synthetic methods. Up to date, most of Cu/Au bimetallic nanostructured materials have been prepared by electrodeposition for both basic and applied electrochemical research. The initial electrodeposition of bulk rather than monolayer deposits of Cu allows the preparation of bimetallic catalysts that have a noble metal core and a non-noble metal-containing shell and the study of pure electronic effects of the latter on the former. For example, electrochemical deposition of nanostrucured copper materials in a reproducible and controllable manner with potential applications in the molecular-scale electronics has recently been reported [5, 6]. The aim of this work is to obtain a nanometer-sized separation that enables electrical contact between the two electrodes via tunneling either directly or after incorporation of an appropriate molecule into a gap.

Underpotential deposition (UPD) of monolayer or multilayer of foreign metal adatoms onto the substrate surface at a potential more positive than the Nernst potential, where bulk deposition takes place, has been extensively studied for decades, due to the stronger bond between the foreign metal adatoms with the metal substrate as compared to the same type substrate [7, 8]. This strategy is not only very important to researchers in surface chemistry for better understandings on the initial electrodeposition process, but also allows precise and reproducible control of the amount of the foreign metal adatoms on the substrate and are suitable for the study of surface coverage dependence of various systems [7]. UPD of a Cu atomic layer on the Au nanoprism thin films electrodes for electro-oxidation of methanol has been explored by Feng et al. [9]. The controllable growth of ultrathin copper films by surface limited redox replacement on Au was also investigated by N. Dimitrov and co-workers [10].

The investigation on glucose electro-oxidation has been a subject of concern for decades since it plays very important roles in developing amperometric glucose sensor for fast monitoring of blood sugar for the treatment and control of diabetes. Most studies on glucose electro-oxidation have involved the use of the glucose oxidase enzyme, a redox protein that catalyzes the oxidation of glucose to gluconolactone. However, most enzymatic-glucose sensors suffer from the serious problems of lack of stability due to the intrinsic nature of enzyme, as well as the significant interferences resulting from the electroactive coexisting species such as ascorbic acid in amperometrically or voltammetrically clinical analysis. Over the last decades, numerous studies have been conducted to alleviate the drawbacks of enzymatic glucose sensors [11–14], in which, some efforts have been made to overcome the interference of ascorbate by employing a permselective membrane to minimize the access of interference substance to the electrode surface. In another strategy, typical electron transfer mediators were utilized to transport electrons between glucose and electrode without using enzymes for overcoming the stability problem of biosensor [15–20]. Recently, various electrode materials have been explored as electron transfer mediators for glucose oxidation. For instance, ordered mesoporous carbon electrode materials were prepared by Guo's research group for nonenzymatic glucose determination [21]. Transition metal oxides such as porous microcubic cuprous oxide and NiO were explored and dispersed in Nafion and multi-walled carbon nanotube respectively for nonenzymatic sensors [22, 23]. Noble metals were also utilized as electrode materials toward glucose oxidation. For instance, Su et al. fabricated a glucose sensor based on highly dispersed Pt nanoparticles supported onto mesoporous carbon [24], Li and co-workers synthesized urchin-like gold submicrostructures by a seed-method and constructed a fast response glucose sensor [25], Hu et al. prepared dihexadecyl hydrogen phosphate capped gold nanoparticle film on a glass carbon electrode and applied to glucose nonenzymatic sensing [26].

One of our research interests focuses on exploiting novel electrocatalytic electrode surfaces for sensor fabrication. In our previous works, PVP-functionalized Cu nanoparticles [27], electrospun CuO nanofibres [28], Cu/titanate intercalation compounds [29], Cu/self-assembled CNT films [30] have been synthesized and explored as catalytic electrode materials for glucose sensor fabrication. Results suggest that Cu-based nanostructured films are promising electron transfer mediator for glucose electro-oxidation in sensor fabrication. In one of our recent works, a sensor for determination of ascorbic acid was successful constructed

by using the ferrocene-functionalized gold nanoparticles as building block, in which, the configuration of GNP not only effectively facilitated the charge transport within the films through the gold nanoparticle cores, but also amplified AA catalytic current by the three-dimensional linked catalytic ferrocene moieties in the assembly [31]. In this work, we demonstrated the preparation of Cu/GNPs bimetallic nano-structured films by controllable potential electrodeposition of copper on the GNPs hydrogen-bonded template for glucose sensor fabrication. The GNPs template was constructed on the surface of glassy carbon electrode based on the hydrogen-bonding interactions between pyridine groups on GNPs surface and carboxyl groups of PAA. The interest in exploring practical Cu/GNPs bimetallic nanostructured glucose sensor was fascinated by the possible synergic effects of the bimetallic nanostructured films in electrocatalysis. The activity of Cu/GNPs films electrode towards glucose electro-oxidation and its sensing performances were evaluated by cyclic voltammetry (CV) and chronoamperometry (I-t). Cu-based bimetallic nanostructured catalysts prepared by bulk electrodepositon of copper on the GNPs hydrogen-bonded template were also investigated.

Experimental

Reagents

Poly(4-vinylpyridine) (PVP), poly(acrylic acid) (PAA) and poly(allylamine hydrochloride) (PAH) were purchased from Sigma-Aldrich (www.sigmaaldrich.com). Copper sulfate ($CuSO_4$), sulfuric acid (H_2SO_4) and perchloric acid ($HClO_4$) were purchased from Shanghai Chemical Reagent Company (Shanghai, China, www.scrri.com). The carbohydrates including D-glucose and others, oxalic acid (OA), ascorbic acid (AA), uric acid (UA), ethanol, sodium hydroxide (NaOH) and the rest inorganic chemicals were purchased from Sinopharm Chemical Reagent Beijing Co. Ltd. (Beijing, China, www.crc-bj.com). All chemicals were of analytical grade and used as received. All solutions were prepared with redistilled water before experiments.

Apparatus

Electrochemical experiments were performed with a CHI660A (CH instruments, USA) electrochemical station in a conventional three-electrode cell under nitrogen atmosphere at room temperature. Bare or modified glassy carbon electrode (GCE), platinum (Pt) wire, and a standard Ag/AgCl electrode (saturated KCl) were used as the working (WE), counter (CE), and reference (RE) electrodes. The pH value was measured by a pH meter (pH211, USA). The morphologies of the materials were observed by scanning electron microscopy (SEM) (SSX-550, Shimadzu, Japan). UV absorption spectra were measured on a Shimadzu UV-2501 spectrophotometer.

Preparation of GNPs with pyridine group tailored surfaces

GNPs with surface-confined functional groups of pyridine were prepared as previous reported [32]. Briefly, 148.8 mg of PVP with molecular weight of 160 K were dissolved in 150 mL of methanol. 70.8 mg of $HAuCl_4$ in 10 mL of methanol was then added under rapid stirring. The molar ratio of metal salts to pyridine units was about 1:2. After 10 min, 27 mg of $NaBH_4$ in 10 mL of methanol was added quickly with the color of mixture changed from yellow to pink immediately, indicating the formation of GNPs. Additional stirring for 30 min leading to the temperature of the Au colloid to room temperature, and the GNPs encapsulated by PVP were thus prepared.

Fabrication of the self-assembled GNPs films on the GCE surface and electrodeposition of copper

The synthesis of GNPs in the presence of PVP resulted in pyridine group tailored surfaces, allowing alternating deposition with PAA based on the hydrogen-bonding interactions between pyridine groups on the surface of GNPs and carboxyl groups at the free ends of polyelectrolyte PAA. Before construction of the hydrogen-bonding GNPs films on the GCE surface, the GCE was polished on emery paper with 1.0, 0.3 and 0.05 μm alumina powder, rinsed thoroughly with ultrapure water and ethanol between each polishing step, and then washed successively with ultrapure water in ultrasonic bath. Immersing the GCE into a polycationic PAH solution (1 wt.%), the NH^{3+}-tailored surface was created. The PAH-pretreated GCE was subsequently immersed in a PAA (1.0 g L^{-1}) methanol solution for 15 min, resulting in a carboxyl-tailored surface. After thoroughly washed with methanol, the GCE was transferred into a methanol solution of GNPs for another 15 min, GNPs with PVP capping layer were adsorbed based on the hydrogen-bonding interactions between pyridine groups on GNPs surface and carboxyl groups of PAA, as depicted in Scheme 1. In this study, multilayer films with five repetitive deposition cycles of GNPs were obtained by repeating the last two steps. GNPs hydrogen-bonded films for SEM and UV characterization were similarly prepared on the indium tin oxide (ITO) surface. The procedure of copper deposition was also shown in Scheme 1. The Cu/GNPs film electrode was prepared by depositing copper particles in the self-assembled GNPs microstructure by electrodeposition in 0.1 M H_2SO_4 solution containing 1 mM $CuSO_4$. The electrochemical behavior and catalysis for glucose of the Cu/GNPs electrode were investigated in

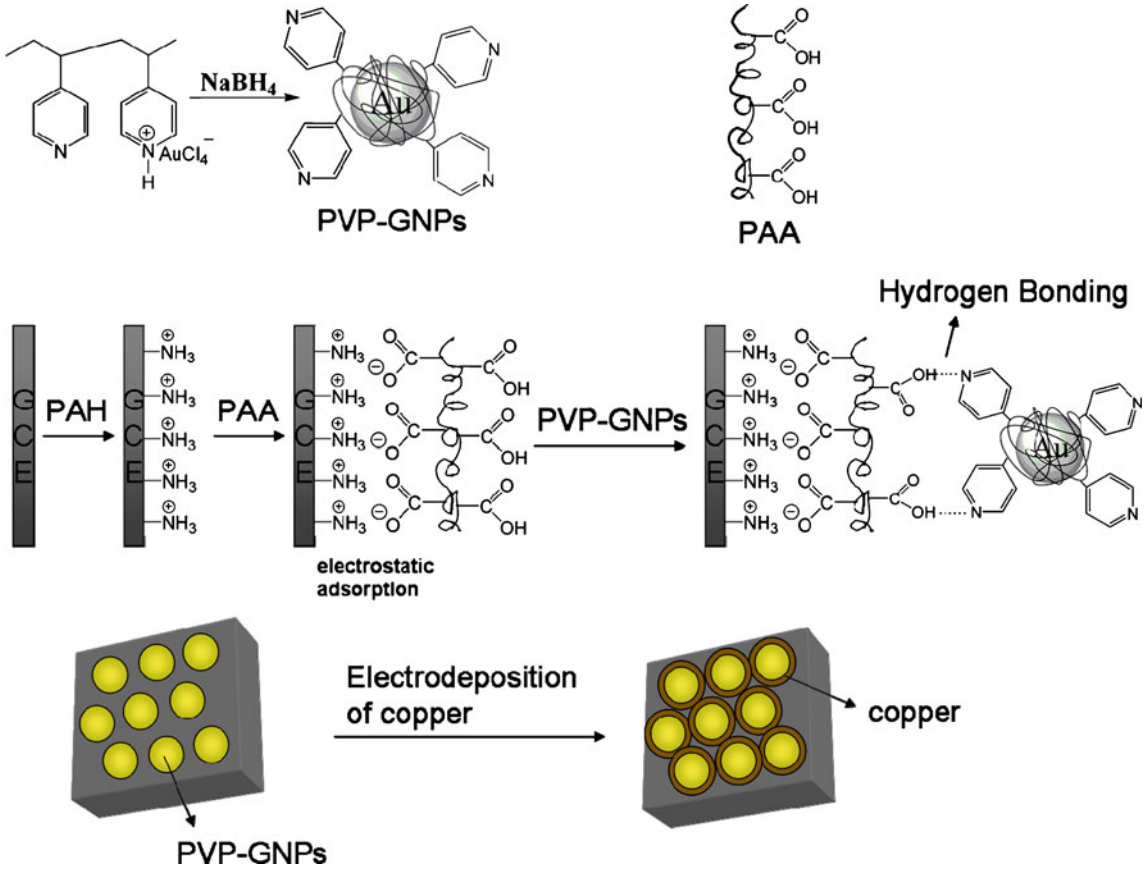

Scheme 1 Schematic representation of the formation of self-assembled GNPs films by hydrogen bonding and the subsequent electrodeposition of copper on the GNPs template

0.2 M NaOH solution (pH=13.0). All the measurements were carried out at room temperature.

Results and discussion

Formation of the GNPs hydrogen-bonded template

The morphology of the GNPs hydrogen-bonded films was observed by SEM. From Fig. 1(a), the GNPs hydrogen-bonded films exhibited representations of homogeneous and closely packed GNPs with uniform sizes around 60 nm (Fig. 1a inset). The typical absorption spectra of GNPs' hydrogen bonding films were measured and shown in Fig. 1(b). Broad absorption bands were observed around 545 nm in the GNPs films, which were in accordance with the plasma adsorption peak of the GNPs solution (Fig. 1b inset).

FTIR spectroscopy characterization of pure PAA films showed a broad absorption band around 2,930 cm^{-1} and the C = O stretching vibration at 1,636 cm^{-1}. The IR spectrum of GNPs hydrogen-bonding films revealed the typical O–H stretching vibrations appeared at 2,490 and 1,895 cm^{-1}, as well as a less associated state of C = O stretching vibration appeared at 1,681 cm^{-1} than that in pure PAA., similar with those in previous report [32], indicating the formation of the hydrogen bonding between the pyridine groups attached on the GNP core and carboxyl groups along the PAA chain. Above results demonstrated that the as-designed GNPs self-assembled films based on the hydrogen-bonding interactions between pyridine groups on GNPs surface and carboxyl groups of PAA were successfully formed.

Electrodeposition of copper at 0 V on the GNPs hydrogen-bonded template and its voltammetric behavior

Electrochemical deposition was demonstrated a powerful strategy to control the quality and quantity of deposits by simply tuning the deposition rate and growth mechanism at suitable deposition potentials. Figure 2 represented the voltammetric response of 1.0 mM $CuSO_4$ in 0.1 M H_2SO_4 at 5 $mV{\cdot}s^{-1}$ on the GNPs films electrode. In experiment, the scanning potential started initially from +0.4 V and proceeded in the negative direction. When the negative potential was limited to −0.10 V, a couple of small peaks around +0.06 V and +0.25 V were observed on the GNPs

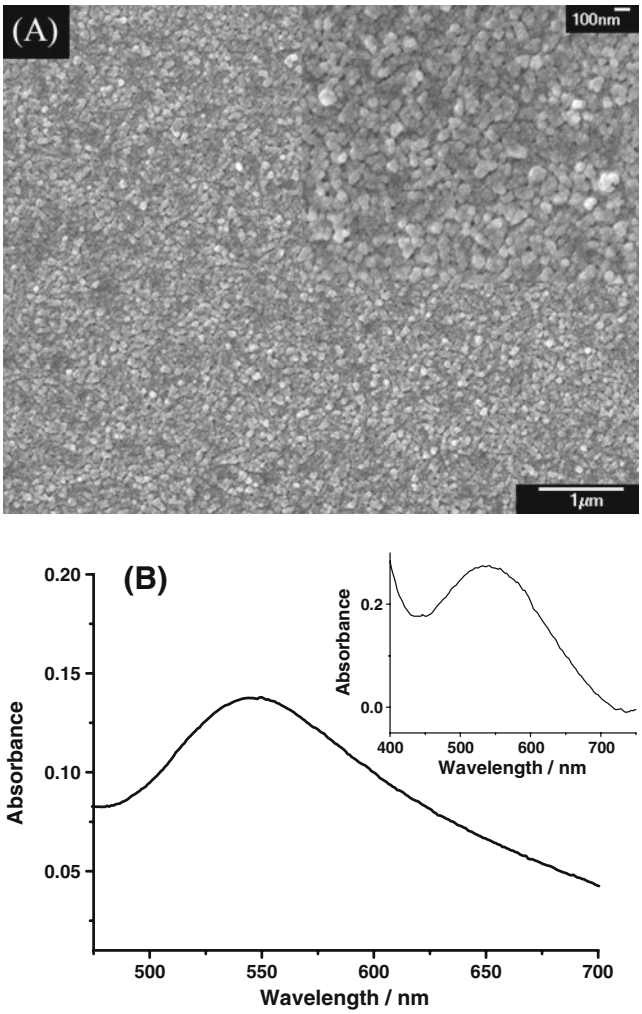

Fig. 1 SEM image (**a**) and UV–vis absorption spectrum (**b**) of the GNPs hydrogen-bonded films. Inset of **b** shows the absorption spectrum of GNPs in methanol solution

films (Fig. 2 curve a). When the potential was scanned towards more negative potential value, for example −0.15 V (Fig. 2 curve b) and −0.20 V (Fig. 2 curve c), respectively, the processes corresponding to the bulk deposition of copper were appeared and the redox currents of bulk deposition/stripping of copper at −0.14 V and +0.07 V increased with the negative shift of potential limitation. The small peaks appeared around +0.06 V and +0.25 V in Fig. 2 (curve a) were ascribed to the processes of precise control growth of copper atoms [33] on the GNPs template at lower deposition potential, while the larger reduction peak appeared at more negative potential (−0.14 V) in Fig. 2 (curve c) corresponded to the processes of bulk deposition of copper. In this work, precise control of the electrochemical growth of Cu on GNPs template was firstly demonstrated in 0.1 M H_2SO_4 containing 1 mM $CuSO_4$ at a controlled deposition potential of 0 V. The redox peak currents were found to be increased with increasing deposition time up to 10 min. After that, the peak currents seemed to be saturated. Here, the deposition time of 10 min was selected for enough quantity of Cu deposited on GNPs films for catalysis. Fig. S1 (Supplementary Material) shows the cyclic voltammetric behavior of Cu growth on the GNPs films at 0 V (deposition time 10 min) in 0.1 M H_2SO_4 containing 1.0 mM $CuSO_4$ at 5 $mV{\cdot}s^{-1}$.

In our experiment, obviously morphological change of the GNPs films before and after electrodeposition of Cu at 0 V in 0.1 M H_2SO_4 solution containing 1.0 mM $CuSO_4$ were not discernable by SEM characterization. The Cu growth on GNPs template also exhibited homogeneous and closely-packed representations, with the size of particles similar with that of GNPs in the template before deposition.

Under same conditions (deposition at 0 V for 10 min in 0.1 M H_2SO_4 solution containing 1.0 mM $CuSO_4$), electrodeposition experiment was also performed on a GCE without the GNPs template. Similar redox features of the GCE without GNPs template before (a) and after (b) electrodeposition of Cu were obtained, as demonstrated by Fig. S2 (Supplementary Material), indicating that Cu could not deposit directly on the surface of GCE at a lower deposition potential of 0 V and the GNPs template plays a very important role in the precise control of Cu growth at 0 V.

Figure 3(a) illustrates the cyclic voltammogram of Cu deposits on GNPs template (0 V, 10 min) in 0.2 M NaOH

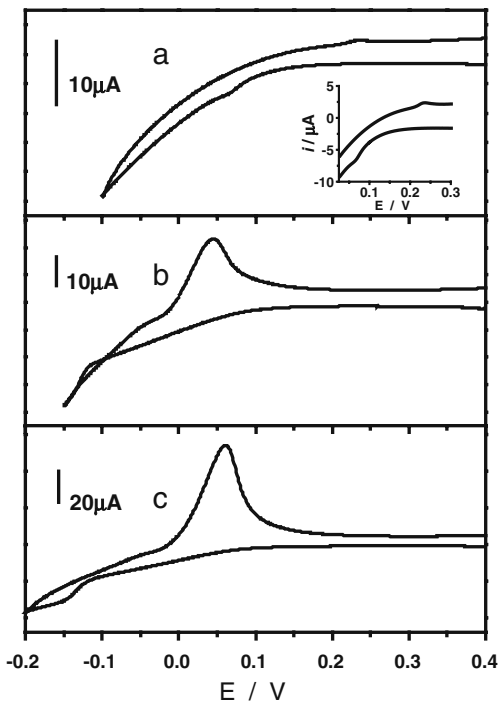

Fig. 2 Cyclic voltammograms of the GNPs films in 0.1 M H_2SO_4 containing 1 mM $CuSO_4$ at 5 $mV{\cdot}s^{-1}$, with the initial potential started from +0.4 V to the negative limitation potential of −0.1 V (**a**), −0.15 V (**b**), −0.2 V (**c**)

aqueous solution in the potential range of −0.6 V to +0.8 V at 50 mV·s^{-1}. Deposition of Cu on the GNPs template resulted in obvious change in the cyclic voltammetric behavior. Compared with that of the GNPs films, deposition of copper at 0 V resulted in a decrease of the double layers current and displayed a broad anodic wave between +0.4 V to +0.6 V and three defined cathodic peaks in the negative potential regions. The broad anodic wave between +0.4 V to +0.6 V was probably associated with the overlapping of the Cu(II)/Cu(III) transition and the formation of gold oxide in the GNPs films during the positive potential scanning. Upon the reverse scan, the small cathodic peaks around −0.2 V and −0.4 V were probably related with the redox transition between the multiple Cu species, and the cathodic peak around 0 V might be ascribed to the reduction process of GNPs oxide. The shape of the cyclic voltammograms at the bimetallic nanostructured films is very similar to that of the electrodeposited Cu on the Au substrate [34], and minor differences could be attributed to the microstructures of deposits prepared on different underlying gold substrates.

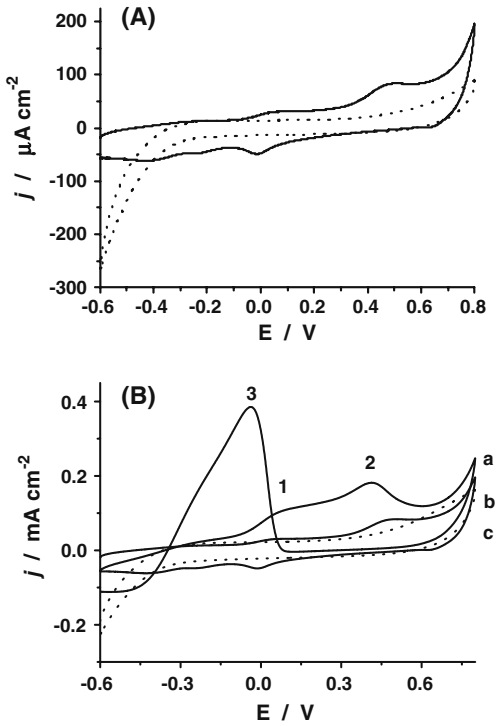

Fig. 3 **a** Cyclic voltammograms of Cu ad-atoms on the GNPs template (0 V, 10 min, 0.1 M H_2SO_4 containing 1.0 mM $CuSO_4$) in 0.2 M NaOH at 50 mV·s^{-1}, the *dot line* shows GNPs modified electrode in 0.2 M NaOH at 50 mV·s^{-1}. **b** Cyclic voltammograms of Cu ad-atoms on the GNP template in 0.2 M NaOH solution with (**a**) and without (**b**) 12 mM glucose at 50 mV·s^{-1}, curve (c) (the *dot line*) is GNPs template in 0.2 M NaOH containing 12 mM glucose

Electro-oxidation of glucose at Cu ad-atoms on the GNPs template

Figure 3(b) (curves a and b) illustrated the dramatic changes in voltammetric profile of Cu growth at 0 V on GNPs template upon addition of 12 mM glucose to 0.2 M NaOH solution. The voltammetric behavior of the GNPs films upon glucose oxidation was also given in the figure for comparison. No obvious oxidation process of glucose was observed on the GNPs films (curve c), while upon Cu deposition, catalytic oxidation of glucose started at negative potentials with two obvious oxidative peaks at around +0.06 V (peak 1) and +0.42 V (peak 2) respectively during the anodic scanning. During the reverse scanning, another oxidative peak appeared at around −0.03 V (peak 3). All peak currents increased linearly with the increases of the glucose concentration, as illustrated in Fig. S3. Compared with that of the gold metal electrode, the potentials for glucose electrocatalytic oxidation on the bimetallic nanostructure films were negatively shifted.

The dramatically enhancement of the catalytic activity by Cu deposits on the GNPs template were attributed to the synergistic catalytic effect of the ad-atoms of Cu growth on GNPs surfaces in the hydrogen bonding GNPs films. The GNPs hydrogen-bonded template was envisioned as an ensembly of closely-packed GNPs interlaced with the dielectric polymeric chains, and behaved totally different from the Au metal, contributing to the lack of obvious electrocatalytic activity towards glucose oxidation. Upon Cu deposition, the organic chains attached onto the GNPs surfaces were removed and Cu/Au bimetallic catalytic sites became more active. An important step in the electrochemical oxidation of carbohydrates is their interaction with the hydroxide/oxide layer on the electrode surface. It has been demonstrated that in basic media, a gold/copper surface gets covered with a layer of bimetallic hydroxide surface formed at potentials considerably below those required for the onset of gold oxide and copper oxide. This coverage of bimetallic hydroxide surface allows an efficient interaction between the hydroxyl groups of the analyte, likely through hydrogen bridges [35–37]. Such favorable interactions between bimetallic hydroxide surface and glucose most likely contribute to the synergistic effects during the electro-oxidation of glucose.

Amperometric determination of glucose and interferential analysis at Cu ad-atoms on the GNPs template

Amperometric analysis was carried out at the bimetallic films of Cu deposites on GNPs. The applied potential for glucose detection was selected at −0.03 V based on the considerations of both sensitivity and the interference effect. By consecutive injection of glucose to 0.2 M NaOH,

very fast, stable and reproducible amperometric responses were observed in Fig. 4(a). The time required to reach the steady state current was about 1 s, which is much faster than those recently reported [27–30, 38]. The *RSD* of the steady state currents for seven individually repetitive tests of 0.1 mM glucose was 2.2%, demonstrating a good reproducibility of the film electrode. The poisoning possibility of chloride ions to the activity of the sensor in glucose determination was examined by adding 0.2 M NaCl to 0.2 M NaOH solution in measurement, results indicated that Cl^- did not cause observable interference in the designated concentration of glucose. The interferential tests of other co-existed interferences, such as ascorbic acid (AA), uric acid (UA), ethanol and oxalic acid (OA) were also carried out by adding 0.002 mM AA, UA, ethanol and OA to 0.2 M NaOH solution containing 0.2 M NaCl and 0.1 mM glucose. Results in Fig. 4(a) revealed that UA, ethanol and OA did not cause any observable interference in glucose detection,

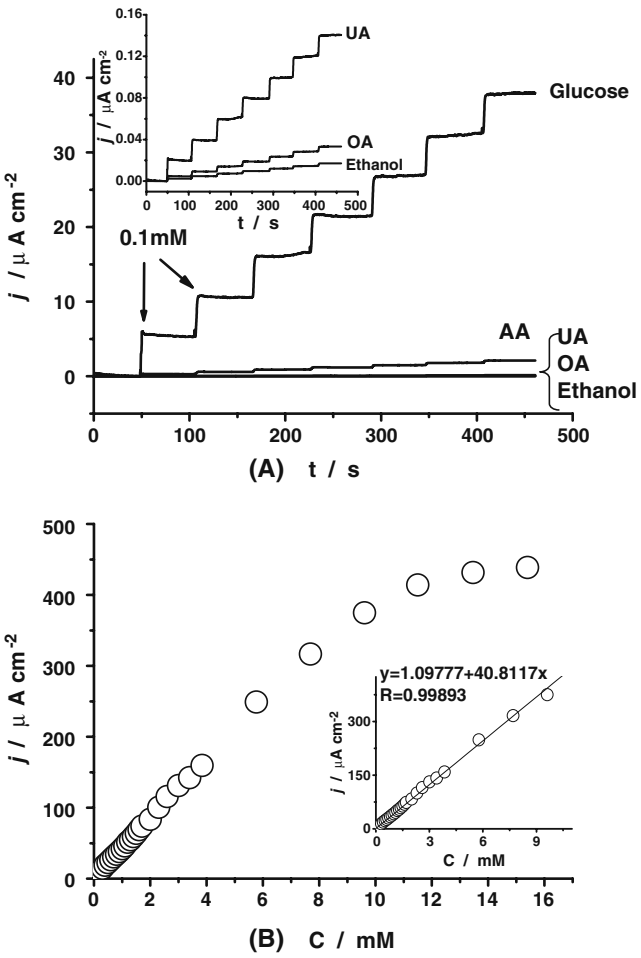

Fig. 4 **a** Amperometric responses of Cu ad-atoms on GNPs template with successive additions of glucose and other interferences to 0.2 M NaOH containing 0.2 M NaCl at −0.03 V. Inset figure shows interference (OA, UA, methanol) effects. **b** Calibration curve for the amperometric response towards glucose

0.02 times of AA caused only neglectable interference, implying a good selectivity of the sensor to glucose.

Figure 4(b) demonstrated a good linear response of the electrocatalytic current of glucose at the film electrode in a wide range of 2.0×10^{-7} M to 1.0×10^{-2} M (correlation coefficient 0.998), and the low concentration parts of which were shown in Fig. S4 and Fig. S5 in Supplementary Material. The detection limit was 5.0×10^{-8} M (signal-to-noise ratio of 3). The current response of the present sensor is 40.8 $\mu A\cdot mM^{-1}\cdot cm^{-2}$, which is 36.1, 2.15, 1.92 and 1.64-fold of 1.13 $\mu A\cdot mM^{-1}\cdot cm^{-2}$ [39], 19 $\mu A\cdot mM^{-1}\cdot cm^{-2}$ [34], 21.23 $\mu A\cdot mM^{-1}\cdot cm^{-2}$ [40] and 24.92 $\mu A\cdot mM^{-1}\cdot cm^{-2}$ of the reported enzymeless sensors [41]. This sensitivity is comparable to that of the Cu/titanate intercalation electrode materials in our recent report [29]. The electrocatalytic stability for glucose oxidation at the films and the reproducibility of the sensor were also evaluated. The current for glucose oxidation decayed 1.95% after 3 months' storage in air, implying a long-term storage stability of the catalytic centers supported on the GCE surface. Under the same fabrication condition, six electrodes were prepared and the *RSD* of the steady state current to 0.03 mM, 5 mM and 8 mM glucose was 3.5%, 4.3% and 4.0% respectively, indicating a satisfied reproducibility of the strategy for sensor fabrication. The *RSD* of the steady state current for six individually repetitive tests of 0.005 mM and 0.6 mM glucose at same films was 2.6%, 5.2% respectively, confirming a good reproducibility of the sensor in determination. Compared analytical features of copper adatoms/GNPs bimetallic nanostructured electrode and some relevant systems in glucose detection recently reported were showed in Table 1. Comparison with the time-consuming chemical synthesis route, the electrodeposition method (including ours) was more facile and cost effective, due to avoiding the subsequent multiple separation procedures necessary for removing the by-products in chemical synthesis. The potential applied for our sensor was more negative, detection limit was lower, liner range was wider than others, although the sensitivity of 40.8 $\mu A\cdot mM^{-1}$ was medium.

Standard glucose samples were detected by using the standard addition method to verify the reliability of the sensor. The determinations were measured at −0.03 V in 0.2 M NaOH and the results were listed in Table S1 (Supplementary Material). The values determined were satisfactory with a good recovery, revealing the reliability of the Cu ad-layers on the GNPs films for glucose determination.

Electro-oxidation of glucose at the film electrodes prepared by bulk electrodeposition of Cu on GNPs hydrogen-bonded template

Experiments of bulk electrodeposition of Cu on GNPs hydrogen-bonded template were also carried out at −0.3 V

Table 1 Figures of merits of comparable methods for direct electrochemical determination of glucose

Reagents used	Methods	E_a	Detection limit	Linear range (mM)	Sensitivity	neglectable interferents compared with glucose	pH	Cost	Reference
AuCu/CNT/C	Electrodeposition	0.34 V	4 μM	0.08–9.26	22 μA·mM^{-1}	0.02 times AA 0.10 times UA	13.0	High	[42]
NiO–Ag NFs/GCE	Chemical synthesis and casting	0.60 V	0.72 μM	~2.63	170.2 μA·mM^{-1}	0.03 times AA 0.08 times UA	13.0	Middle	[43]
MWCNT/PEI/Cu	Chemical synthesis and casting	0.35 V	0.5 μM	0.01–0.3	50.47 μA·mM^{-1}	0.02 times AA 0.02 times UA	12.3	Middle	[44]
Cu/CuO nanowire	Chemical synthesis and casting	0.30 V	50 μM	0.1–12	8.59 μA·mM^{-1}	0.05 times AA 0.05 times UA	13.0	Low	[45]
Cu/GNPs	Cu underpotential deposition on GNPs	−0.03 V	0.05 μM	0.0002–10	40.8 μA·mM^{-1}	0.02 times AA 0.02 times OA 0.02 times UA 0.02 times ethanol	13.0	Middle	This work

for sufficient loading of Cu on the GNPs films, and its performances in glucose electro-oxidation were also investigated. Figure 5(a) presented the voltammetrically catalytic responses of the electrode prepared by bulk electrodeposition of Cu at −0.3 V on GNPs template. Glucose oxidation were observed at the sites related with both gold and copper surfaces as revealed by the oxidation peaks at −0.26 V, −0.03 V and +0.65 V, representing combined intrinsic catalytic characteristics of Cu and Au in the films. Spherical Cu deposits were uniformly dispersed on the GNPs template in the low resolution SEM image (Fig. 5b). High resolution image exhibited regular nanoflowers with diameter of ca. two micrometers (inset in Fig. 5b). Bulk electrodeposition of Cu on GNPs hydrogen-bonded template demonstrated perfectly electrocatalytic activity to glucose oxidation by increasing the glucose oxide current up to 39.47% than that of the bulky deposited copper on the bare GCE.

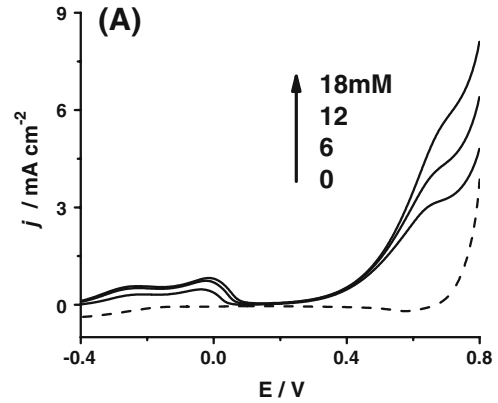

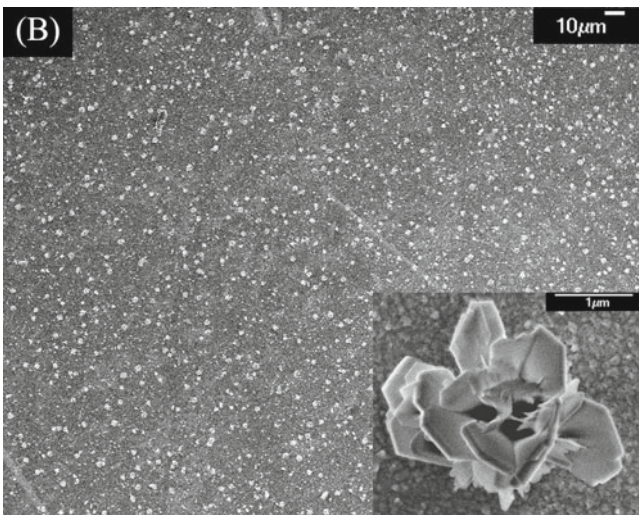

Fig. 5 **a** Voltammograms of bulk electrodeposition of Cu on GNPs hydrogen-bonded template in 0.2 M NaOH solution containing different concentration of glucose at 50 mV·s^{-1}. **b** SEM image of the GNPs bulk electrodeposition of Cu on GNPs hydrogen-bonded template

Conclusions

Defined bimetallic nanostructured electrode for sensor application were achieved by controlling deposition of Cu adatoms at 0 V on the closely packed GNPs self-assembled template constructed on the surface of glassy carbon electrode based on the hydrogen-bonding interactions between pyridine groups on GNPs surface and carboxyl groups of PAA. The interest in exploring practical Cu/GNPs bimetallic nanostructured sensor was fascinated by its synergic effects in electrocatalysis. Electrochemistry and electrocatalysis of the Cu adatoms on the GNPs template towards glucose electro-oxidation in alkaline media were evaluated by cyclic voltammetry and chronoamperometry in detail. Results revealed that GNPs in the template accelerated the Cu ad-atoms electrodeposition at low deposition potential, and the resulting Cu/GNPs films exhibited synergistic catalytic effect towards glucose oxidation. Cu-based bimetallic nanostructured catalysts prepared by bulk electrodepositon of copper at −0.3 V on the GNPs hydrogen-bonding template were also investigated. Electrochemical combination of noble metal and transition metal nanostructures provides good opportunities for fabricating novel and high performance sensors and devices.

Acknowledgement This work was supported by National Natural Science Foundation of China under Grants 20543003 and 21075048, as well as Scientific Research Foundation for Returned Overseas Chinese Scholars, State Education Ministry of China.

References

1. Wang D, Villa A, Porta F, Prati L, Su DS (2008) Bimetallic Gold/Palladium catalysts: correlation between nanostructure and Synergistic effects. J Phys Chem C 112:8617
2. Teng XW, Wang Q, Liu P, Han WQ, Frenkel A, Wen W, Marinkovic N, Hanson JC, Rodriguez JA (2007) Formation of Pd/Au nanostructures from Pd nanowires via galvanic replacement reaction. J Am Chem Soc 130:1093
3. Kurniawan F, Tsakova V, Mirsky VM (2006) Gold nanoparticles in nonenzymatic electrochemical detection of sugars. Electroanal 18:1937
4. Kambayashi M, Zhang JD, Oyama M (2004) Crystal growth of gold nanoparticles on indium tin oxides in the absence and presence of 3-mercaptopropyl-trimethoxysilane. Cryst Growth Des 5:81
5. Chen F, Qing Q, Ren L, Tong LM, Wu ZY, Liu ZF (2007) Formation of nanogaps by nanoscale Cu electrodeposition and dissolution. Electrochim Acta 52:4210
6. Meszaros G, Kronholz S, Karthauser S, Mayer D, Wandlowski T (2007) Electrochemical fabrication and characterization of nanocontacts and nm-sized gaps. Appl Phys A 87:569
7. Gregory BW, Stickney JL (1991) Electrochemical atomic layer epitaxy (ECALE). J Electroanal Chem 300:543
8. Herrero E, Buller LJ, Abruna HD (2001) Underpotential deposition at single crystal surfaces of Au, Pt, Ag and other materials. Chem Rev 101:1897
9. Li WJ, Ma HY, Zhang JT, Liu XY, Feng XL (2009) Fabrication of gold nanoprism thin films and their applications in designing high activity electrocatalysts. J Phys Chem C 113:1738
10. Viyannalage LT, Vasilic R, Dimitrov N (2007) Epitaxial growth of Cu on Au(111) and Ag(111) by surface limited redox replacement an electrochemical and STM study. J Phys Chem C 111:4036
11. Hoshi T, Saiki H, Kuwazawa S, Tsuchiya C, Chen Q, Anzai J (2001) Selective permeation of hydrogen peroxide through polyelectrolyte multilayer films and its use for amperometric biosensors. Anal Chem 73:5310
12. Xu F, Wang L, Gao MN, Jin LT, Jin JY (2002) Amperometric sensor for glucose and hypoxanthine based on a Pd–IrO2 modified electrode by a co-crosslinking bienzymic system. Talanta 57:365
13. Krikstopaitis K, Kulys J, Tetianec L (2004) Bioelectrocatalytical glucose oxidation with phenoxazine modified glucose oxidase. Electrochem Commun 6:331
14. Pandey PC, Upadhyay S, Shukla NK, Sharma S (2003) Studies on the electrochemical performance of glucose biosensor based on ferrocene encapsulated ORMOSIL and glucose oxidase modified graphite paste electrode. Biosens Bioelectron 18:1257
15. Beden B, Largeaud F, Kokoh KB, Lamy C (1996) Fourier transform infrared reflectance spectroscopic investigation of the electrocatalytic oxidation of D-glucose: identification of reactive intermediates and reaction products. Electrochim Acta 41:701
16. Sun YP, Buck H, Mallouk TE (2001) Combinatorial discovery of alloy electrocatalysts for amperometric glucose sensors. Anal Chem 73:1599
17. Bae IT, Yeager E, Xing X, Liu CC (1991) In situ infrared studies of glucose oxidation on platinum in an alkaline medium. J Electroanal Chem 309:131
18. Wittstock G, Strubing A, Szargan R, Werner G (1998) Glucose oxidation at bismuth-modified platinum electrodes. J Electroanal Chem 444:61
19. Park S, Chung TD, Kim HC (2003) Nonenzymatic glucose detection using mesoporous platinum. Anal Chem 75:3046
20. Shoji E, Freund MS (2001) Potentiometric sensors based on the inductive effect on the pK_a of poly(aniline): a nonenzymatic glucose sensor. J Am Chem Soc 123:3383
21. Ndamanisha JC, Guo LP (2009) Nonenzymatic glucose detection at ordered mesoporous carbon modified electrode. Bioelectrochem 77:60
22. Zhang L, Ni YH, Li H (2010) Addition of porous cuprous oxide to a nafion film strongly improves the performance of a nonenzymatic glucose sensor. Microchim Acta 171:103
23. Xie SF, Xiang BR, Zhang M, Deng HS (2010) A highly sensitive nonenzymatic glucose sensor based on NiO-modified multi-walled carbon nanotubes. Microchim Acta 168:259
24. Su C, Zhang C, Lu GQ, Ma C (2010) Nonenzymatic electrochemical glucose sensor based on Pt nanoparticles/mesoporous carbon matrix. Electroanal 22:1901
25. Xu FG, Cui K, Sun YJ, Guo CL, Liu ZL, Zhang Y, Shi Y, Li Z (2010) Facile synthesis of urchin-like gold submicrostructures for nonenzymatic glucose sensing. Talanta 82:1845
26. Zhao J, Yu JJ, Wang F, Hu SS (2007) Fabrication of gold nanoparticle-dihexadecyl hydrogen phosphate film on a glassy carbon electrode, and its application to glucose sensing. Microchim Acta 156:277
27. Liu HY, Su XD, Tian XF, Huang Z, Song WB, Zhao JZ (2006) Preparation and electrocatalytic performance of functionalized copper-based nanoparticles supported on the gold surface. Electroanal 18:2055
28. Wang W, Zhang LL, Tong SF, Li X, Song WB (2009) Three-dimensional network films of electrospun copper oxide nanofibers for glucose determination. Biosens Bioelectron 25:708
29. Tong SF, Jin HY, Zheng DF, Wang W, Li X, Xu YH, Song WB (2009) Investigations on copper-titanate intercalation materials for amperometric sensor. Biosens Bioelectron 24:2404

30. Li X, Zhu QY, Tong SF, Wang W, Song WB (2009) Self-assembled microstructure of carbon nanotubes for enzymeless glucose sensor. Sens Actuators, B 136:444
31. Shi HY, Xu Y, Wang Y, Song WB (2010) Assembly of ferrocenylhexanethiol functionalized gold nanoparticles for ascorbic acid determination. Microchim Acta 171:81
32. Hao EC, Lian TQ (2000) Buildup of polymer/Au nanoparticle multilayer thin films based on hydrogen bonding. Chem Mat 12:3392
33. Ben Aoun S, Dursun Z, Sotomura T, Taniguchi I (2004) Effect of metal ad-layers on Au(111) electrodes on electrocatalytic reduction of oxygen in an alkaline solution. Electrochem Commun 6:747
34. Mohammadi H, Amine A, El Rhazi M, Brett CMA (2004) Copper-modified gold electrode specific for monosaccharide detection: use in amperometric determination of phenylmercury based on invertase enzyme inhibition. Talanta 62:951
35. Bruckenstein S, Shay M (1985) An in situ weighing study of the mechanism for the formation of the adsorbed oxygen monolayer at a gold electrode. J Electroanal Chem 188:131
36. Angerstein-Kozlowska H, Conway BE, Hamelin A, Stoicoviciu L (1987) Elementary steps of electrochemical oxidation of single-crystal planes of Au Part II. A chemical and structural basis of oxidation of the (111) plane. J Electroanal Chem 228:429
37. Vitt JE, Larew LA, Johnson DC (1990) The importance of adsorption in anodic surface-catalyzed oxygen-transfer reactions at gold electrodes. Electroanal 2:21
38. Tong SF, Wang W, Li X, Xu YH, Song WB (2009) Electrochemical preparation of copper-based/titanate intercalation electrode material. J Phys Chem C 113:6832
39. Lee H, Yoon SW, Kim EJ, Park J (2007) In-situ growth of copper sulfide nanocrystals on multiwalled carbon nanotubes and their application as novel solar cell and amperometric glucose sensor materials. Nano Lett 7:778
40. Wang Y, Wei WZ, Zeng JX, Liu XY, Zeng XD (2008) Fabrication of a copper nanoparticle/chitosan/carbon nanotube-modified glassy carbon electrode for electrochemical sensing of hydrogen peroxide and glucose. Microchim Acta 160:253
41. Wang J, Chen G, Wang M, Chatrathi MP (2004) Carbon-nanotube/copper composite electrodes for capillary electrophoresis microchip detection of carbohydrates. Analyst 129:512
42. Liu DY, Luo QM, Zhou FQ (2010) Nonenzymatic glucose sensor based on gold–copper alloy nanoparticles on defect sites of carbon nanotubes by spontaneous reduction. Synth Met 160:1745
43. Ding Y, Wang Y, Su L, Zhang H, Lei Y (2010) Preparation and characterization of NiO–Ag nanofibers, NiO nanofibers, and porous Ag: towards the development of a highly sensitive and selective non-enzymatic glucose sensor. J Mater Chem 20:9918
44. Wu HX, Cao WM, Li Y, Liu G, Wen Y, Yang FH, Yang SP (2010) In situ growth of copper nanoparticles on multiwalled carbon nanotubes and their application as non-enzymatic glucose sensor materials. Electrochim Acta 55:3734
45. Wang GF, Wei Y, Zhang W, Zhang XJ, Fang B, Wang L (2010) Enzyme-free amperometric sensing of glucose using Cu–CuO nanowire composites. Microchim Acta 168:87